Numerical Modeling of the Harmonic Constituents of the Tides, with Application to the English Channel

CHRISTIAN LE PROVOST AND GILLES ROUGIER

Institute of Mechanics, University of Grenoble, France

ALAIN PONCET

Institute of Applied Mathematics, University of Grenoble, France

(Manuscript received 1 August 1980, in final form 4 May 1981)

ABSTRACT

An in-time spectral, finite-element method is proposed for modeling the main astronomical and nonlinear constituents of the tide in any oceanic or shallow-water area. The classical nonlinear hyperbolic problem for long waves is transformed to a set of elliptic modal problems by looking at a multiperiodic solution with basic frequencies deduced from the tide-generating potential development. The method is based on a perturbation technique. Because of the non-analytic formulation of the quadratic bottom friction, a multi-periodic development of these terms is needed. This is realized under a restrictive hypothesis that a dominant wave is present in the studied tidal spectrum. Although the damping terms of friction deduced from this development are of second order, their influence on the real solutions is very important. Thus, a quasi-linearization of these damping terms makes possible a computation of damped solutions, as soon as the first order of approximation, for each wave investigated. Practically, for each order of approximation and each significant frequency, we have to solve a second-order equation of the *Helmholtz* type, which is possible to write under a variational formulation.

A finite-element method is used for the numerical integrations. First, an illustration of the method is presented for the academic case of a wave propagating in a rectangular rotating channel together with its first harmonic produced inside the basin by nonlinear processes. Then a practical application is presented with the computation of some of the main constituents of the tide in the English Channel: the dominant wave M_2 and its first harmonic M_4, and two astronomical constituents, the semidiurnal S_2 and the diurnal K_1. The possibilities offered by the finite-element procedure used appear very attractive for practical investigations of oceanic and shallow-water tides. The computing time requirements are small.

1. Introduction

During the last 20 years, in connection with the increase of computer facilities, numerical modeling of tides has been intensively developed and applied everywhere tidal motion dominantly influences currents and sea surface elevation. The number of such numerical models presented in the literature is enormous. Even restricted to a particular area, the European shelf seas for instance, a complete list of such investigations would be difficult to achieve. For example, some representative models are those of Hansen (1962), Hyacinthe and Kravtchenko (1970), Pingree and Maddock (1978) for the English Channel; Prandle (1978) for the Strait of Dover; Nihoul and Ronday (1975) for the Southern Bight; Ramming (1976) for the German Bight; Brettschneider (1967), Martchuk *et al.* (1973), Davies (1976) for the North Sea; Heaps (1974) for the Irish Sea; Flather (1976) for the whole continental shelf, etc.

All these models are based on finite-difference methods (FDM). They have their own characteristics, but generally all of them are modeling only a single tidal period of the real phenomenon or some mean cycle (mean spring tides for instance) because of computer time requirements. These limitations result from two fundamental constraints:

- In order to be precise, these models need refined spatial discretization in shallow-water areas, where nonlinear processes significantly distort tidal waves. As FDM generally use regular grids, this constraint requires very large memory core requirements, when the domain investigated is extended far toward the open sea.
- In order to be stable, small time steps are needed in connection with the well-known Courant-Friedrich-Lewy condition for explicit finite-difference schemes.

During the past decade, a significant number of papers have proposed applying FDM to the resolution of the shallow-water equations, in order to take advantage of the flexibility of the grid networks

0022-3670/81/081123-16$08.00

which can be employed with these techniques. By refining the mesh in very shallow-water areas and using coarser grids offshore, an optimal spatial discretization can be used. The earliest finite-element tidal models were developed by Grotkop (1973), Connor and Wang (1974) and Taylor and Davis (1975). Some applications have been performed by Brebbia and Partridge (1976) for the North Sea, by Wang (1978) for the Massachussets Bay, and by Kawahara and Hasegawa (1978) for the Hamaishi Bay and the Tokyo Bay. However, up to now, direct time-dependent finite-element modeling of tides has been in a phase of careful analysis and criticism (Gray, 1980), especially because of high computer costs.

Recently, another approach to tidal modeling has been investigated simultaneously by some authors (Kawahara *et al.*, 1977; Pearson and Winter, 1977; Le Provost and Poncet, 1977; Jamart and Winter, 1978; Lynch, 1978). The basic idea is that when periodic motions are considered, excessive computer costs resulting from the succession of time-step integration can be avoided by replacing the time-dependent equations of motion by an equivalent set of modal equations corresponding to the significant tidal components present in the real spectrum. Of course, the main difficulties of such an approach are connected with the nonlinearities of the shallow-water equations: advective transport and bottom friction. Different methods can be used to include these nonlinearities in the computations. Thus, in order to avoid analytic Fourier decompositions, Pearson and Winter (1977), for instance, evaluate the nonlinear terms numerically from an iterative process. In contrast, we have developed a complete analytic Fourier expansion of the shallow-water equations, as a preliminary to any numerical computation. But, in any case, the transposition of the problem from the time domain into the spectral domain transforms the hyperbolic time-dependent problem of tidal propagation into a set of elliptic modal problems of the *Helmholtz* type, with suitable boundary conditions. A secondary interest of such a transformation is that a variational formulation can be derived for each of these modal problems. Thus, FEM appear to be the natural way of numerical integration in realistic complex areas.

In a previous paper (Le Provost and Poncet, 1978), an application to the computation of the dominant component of the tides in the English Channel (the semidiurnal M_2 constituent) was presented as a first and simplified illustration of the method. The purpose of this paper is to give a complete description of this in-time spectral method applied to the resolution of the complete nonlinear problem of tide propagation in oceanic and coastal areas: analytical formulation of the equations, general Fourier expansion of the non-analytical friction terms, modal decomposition of the primitive equations and limit conditions, variational formulation of the typical complex second-order *Helmholtz* equation defining each component of the spectrum. As an illustration, the method is first applied to the computation of a sinusoidal tidal wave (such as M_2) and its first harmonic (M_4), propagating in a rectangular rotating channel. As an example of practical application, the determination of the main components of the tides in the English Channel are then presented: M_2, S_2, N_2, M_4, K_1. In the conclusion, some indications of computer costs are given, for comparison with classical FDM, showing a factor of 10 between the two methods. However, it must be noted that such a method cannot be extended too far in very shallow estuaries where nonlinear effects are too large, and the method is not able to compute non-periodic phenomena, such as storm surges.

2. Basic equations and boundary conditions

The analytical and numerical methods presented in this paper are developed in order to compute either oceanic or coastal tides. Consequently, the nonlinear, depth-integrated shallow-water equations are formulated in a spherical coordinate system:

$$\left\{\begin{aligned}
&\frac{\partial u}{\partial t} + \frac{u}{\rho}\frac{\partial u}{\partial \lambda} + \frac{v}{a}\frac{\partial u}{\partial \phi} - \frac{uv}{a}\tan\phi - 2\Omega \sin\phi v \\
&\quad + \frac{Cu}{D}(u^2 + v^2)^{1/2} + \frac{g}{\rho}\frac{\partial \zeta}{\partial \lambda} = \frac{g}{\rho}\frac{\partial P}{\partial \lambda}, \qquad (1a)\\
&\frac{\partial v}{\partial t} + \frac{u}{\rho}\frac{\partial v}{\partial \lambda} + \frac{v}{a}\frac{\partial v}{\partial \phi} + \frac{u^2}{a}\tan\phi + 2\Omega \sin\phi u \\
&\quad + \frac{Cv}{D}(u^2 + v^2)^{1/2} + \frac{g}{a}\frac{\partial \zeta}{\partial \phi} = \frac{g}{a}\frac{\partial P}{\partial \phi}, \qquad (1b)\\
&\frac{\partial \zeta}{\partial t} + \frac{1}{\rho}\frac{\partial}{\partial \lambda}(Du) + \frac{1}{\rho}\frac{\partial}{\partial \phi}(Dv\cos\phi) = 0, \qquad (1c)
\end{aligned}\right.$$

where

λ	longitude
ϕ	latitude
a	earth radius
ρ	radius of latitude circle [$=a\cos\phi$]
t	time
ζ	sea surface elevation
u, v	eastward and northward mean depth velocity components
H	undisturbed depth of water
D	total depth of water [$=H + \zeta$]
Ω	angular velocity of the earth rotation
C	bottom friction coefficient
g	gravity
P	generating tidal potential.

In a domain $\mathcal{D}$ limited by coastal boundaries Γ_1 and open boundaries Γ_2, tidal computations consist in integrating (1) with limit conditions

$$\begin{cases} \mathbf{V}\cdot\mathbf{n} = 0 \quad \text{along } \Gamma_1 \quad [\mathbf{V} = (u, v)], & (2a) \\ \zeta(\lambda, \phi, t) \quad \text{given along } \Gamma_2, & (2b) \end{cases}$$

where $\mathbf{n}$ is the unity vector normal to Γ_1. In (2a) the coast is assumed impermeable, and no flow perpendicular to the coast is therefore permitted; in (2b), the seaward boundary condition is supposed to be available from tide gage data.

3. In-time spectral decomposition of the problem

a. Development of the solution

Darwin (1883) and Doodson (1921), have shown that the spectral structure of the generating tidal potential can be written as

$$P = \sum_{i=1}^{N_p} P_i \cos(\omega_i t + k_i). \quad (3)$$

It contains N_p constituents of precisely defined frequencies ω_i. Although Doodson's development leads to an important number N_p of components, only some of them are practically significant. Table 1 (p. 1135) gives the name, symbol and period of the main classical constituents, with the ratio of their amplitude to that of the major component of each group (semidiurnal and diurnal). It can be noticed that, except for the second S_2, the third N_2 and the fourth K_2, all the others correspond to only some small percentage of the M_2 constituent in the semidiurnal group. Consequently, in areas where the diurnal components are of small amplitude, and this is the case for the European shelf seas for instance, a rather good approximation of the real phenomenon can be described by taking only these four main astronomical constituents (M_2, S_2, N_2 and K_2). In the following, N_p is thus supposed to be reduced to a rather small integer.

Since oceanic tides are linear, it can be assumed that in the ocean, the vector solution $S(u, v, \zeta)$ can be developed in the form

$$S = \sum_{i=1}^{N_p} A_i S_{i1} = \sum_{i=1}^{N_p} A_i s_{i1}(\lambda, \phi) \cos[\omega_i t + g_i(\lambda, \phi)], \quad (4)$$

where A_i is a characteristic amplitude of the wave of index i.

In coastal areas, nonlinear phenomena introduce new frequencies in the tidal spectrum. These processes can be formulated analytically by using a perturbation method in which the complete solution in a coastal basin is assumed to be of the form

$$S = \sum_{i=1}^{N_p} (A_i S_{i1} + \sum_{p=1}^{\infty} A_i^p S_{ip}) + \sum_{i=1}^{N_p} \sum_{l=1}^{N_p} A_i A_l S_{il11} + \cdots, \quad i \neq l, \quad (5)$$

with solutions S_{ip}, and S_{il11} expressed as

$$S_{ip} = s_{ip} \cos[(a\omega_1 + b\omega_i)t + g_{ip}],$$

$$S_{il11} = s_{il11} \cos[(a\omega_1 + b\omega_i + c\omega_l)t + g_{il11}],$$

with a, b, and c integers. They correspond to nonlinear harmonic constituents of the astronomical waves coming from the ocean and to nonlinear wave-wave interactions between these N_p components. Theoretically, development (5) includes an infinite number of terms, but practically, it can be limited, especially if the domain $\mathcal{D}$ does not include very shallow estuarine areas (Le Provost, 1974).

As a consequence from developments (4) and (5), the limit conditions (2) are expressed under the form (4) if the open boundary Γ_2 is situated in the ocean, or the form (5) if Γ_2 is in a coastal area.

b. Development of quadratic friction term

The classical perturbation method consists of introducing expansion (5) in Eq. (1), and identifying the same orders of magnitude in A_i^p and $A_i A_1$. Given the non-analytical formulation of the quadratic bottom friction, it is necessary to expand it beforehand under a form similar to (5). This development has been presented by Le Provost (1973). It assumes that the velocity field is expressed as

$$\begin{cases} u = \sum_{k=1}^{N_c} A_k u_k \cos(\omega_k t + \psi_k) \\ v = \sum_{k=1}^{N_c} A_k v_k \cos(\omega_k t + \chi_k). \end{cases} \quad (6)$$

with N_c being the number of constituents of frequency ω_k and of order of magnitude A_k present in the velocity spectrum. It is valid only in areas where a dominant wave can be found of amplitude much larger than the others, such that

$$u_1^2 + v_1^2 \neq 0$$

$$A_1^2(u_1^2 + v_1^2) \gg \sum_{k=2}^{N_c} (u_k^2 + v_k^2), \quad (7)$$

with 1 being the index of the dominant wave.

The two components of the friction vector are expanded as follows:

$$\begin{cases} F_x = \dfrac{Cu}{D}\sqrt{u^2+v^2} \\ \quad = \dfrac{C}{H}\sum_{k,l} A_k A_l \sum_n FX_{kl}^{(n)} \cos[\Omega_{kl}^{(n)} t + \Phi X_{kl}^{(n)}] \\ F_y = \dfrac{Cv}{D}\sqrt{u^2+v^2} \\ \quad = \dfrac{C}{H}\sum_{kl} A_k A_l \sum_n FY_{kl}^{(n)} \cos[\Omega_{kl}^{(n)} t + \Phi Y_{kl}^{(n)}] \end{cases} \tag{8}$$

where $\Omega_{kl}^{(n)} = \sum_{m=1}^{N_c} p_m(k, l, n)\omega_m$, $p_m \epsilon$ integer ≥ 0, and $FX_{kl}^{(n)}$, $FY_{kl}^{(n)}$, $\Phi X_{kl}^{(n)}$, $\Phi Y_{kl}^{(n)}$ are functions of u_k, v_k, ψ_k, χ_k. These functions have been determined analytically for the orders of approximations A_1^2, $A_1 A_k$, and A_k^2 ($k = 2, 3, \ldots N_c$). Some of these analytical expressions will be presented later.

The identification of the frequencies $\Omega_{kl}^{(n)}$ corresponding in (8) to these different orders of approximation gives

(i) at order A_1^2: pulsations $(2n + 1)\omega_1$ (9a)

(ii) at order $A_1 A_k$: pulsations $2n\omega_1 + \epsilon\omega_k$ (9b)

with $n = 0, 1, 2 \ldots \infty$, and $\epsilon = \pm 1$.

Eq. (9) can be interpreted as follows:

1) For $n = 0$, we find the pulsations constituting the velocity spectrum: ω_1 at the order A_1^2, ω_k at the order $A_1 A_k$. The corresponding terms of (8) represent the damping effect of friction.

2) For $n \neq 0$ in (9), all the pulsations appearing are representative of harmonics or wave-wave interactions induced by quadratic bottom friction.

c. *Linearization of the damping terms of bottom friction*

Since bottom friction is formulated following the quadratic Chezy law, its effects can be taken into account only at the second order of approximation in the classical perturbation method, the first-order solution corresponding to the linear system deduced from (1) by omitting advective and frictional terms. But this first-order approximation appears to be very far from the real solution, because of the importance of bottom friction damping: this point has been shown recently by Kabbaj and Le Provost (1980). In their paper, it was proposed to adapt the perturbation method in order to take into account the damping terms of bottom friction of order A_1^2 as soon as the first-order A_1 for the dominant wave, and of order $A_1 A_k$ at the order A_k for the other components of A_k magnitude. Such a method corresponds to a quasilinearization of the damping part of bottom friction. Its application for a practical case, a channel of constant depth 50 m, leads to satisfying approximate solutions at the second-order of approximation.

We shall follow the same procedure in the present method. Let us consider the damping terms of (8) and deduce their quasi-linearized formulation.

THE DOMINANT WAVE

In the developments of (8) presented by Le Provost (1973), the terms of order A_1^2 corresponding to the frequency ω_1 are

$$\begin{cases} FX_{11}^{(0)} \cos[\omega_1 t + \phi X_{11}^{(0)}] \\ \quad = \dfrac{u_1}{\sqrt{2}}\sqrt{u_1^2 + v_1^2}[G_{00}\cos(\omega_1 t + \psi_1) \\ \qquad + \tfrac{1}{2} G_{02}\cos(\omega_1 t + 2\theta - \psi_1)] \\ FY_{11}^{(0)} \cos[\omega_1 t + \phi Y_{11}^{(0)}] \\ \quad = \dfrac{v_1}{\sqrt{2}}\sqrt{u_1^2 + v_1^2}[G_{00}\cos(\omega_1 t + \chi_1) \\ \qquad + \tfrac{1}{2} G_{02}\cos(\omega_1 t + 2\theta - \chi_1)], \end{cases} \tag{10}$$

with

$$G_{00} = \frac{1}{2\pi}\int_{-\pi}^{+\pi} [1 + J_1 \cos(2\omega_1 t + 2\theta)]^{1/2} d(\omega_1 t + \theta),$$

$$G_{0n} = \frac{1}{\pi}\int_{-\pi}^{+\pi} [1 + J_1 \cos(2\omega_1 t + 2\theta)]^{1/2} \times \cos[n(\omega_1 t + \theta)] d(\omega_1 t + \theta),$$

$$J_1 = 1 - \frac{4u_1^2 v_1^2}{(u_1^2 + v_1^2)^2}\sin^2(\psi_1 - \chi_1),$$

$$\tan 2\theta = \frac{u_1^2 \sin 2\psi_1 + v_1^2 \sin^2 \chi_1}{u_1^2 \cos 2\psi_1 + v_1^2 \cos 2\chi_1}.$$

Eqs. (10) can be written in a slightly different form which corresponds to a quasi-linearization:

$$\begin{cases} A_1^2 FX_{11}^{(0)} \cos[\omega_1 t + \phi X_{11}^{(0)}] = R_1 A_1 u_1 \cos(\omega_1 t + \psi_1) \\ \qquad + \dfrac{R_1'}{\omega_1}\dfrac{\partial}{\partial t}[A_1 v_1 \cos(\omega_1 t + \chi_1)] \\ A_1^2 FY_{11}^{(0)} \cos[\omega_1 t + \phi Y_{11}^{(0)}] = R_1 A_1 v_1 \cos(\omega_1 t + \chi_1) \\ \qquad - \dfrac{R_1'}{\omega_1}\dfrac{\partial}{\partial t}[A u_1 \cos(\omega_1 t + \psi_1)], \end{cases} \tag{11}$$

with

$$R_1 = \frac{A_1}{\sqrt{2}}\sqrt{u_1^2 + v_1^2}\left(G_{00} + \frac{G_{02}}{2J_1}\right),$$

$$R_1' = \frac{A_1}{\sqrt{2}}\sqrt{u_1^2 + v_1^2}\,\frac{\epsilon G_{02}}{2J_1}(1 - J_1^2)^{1/2},$$

$$\epsilon = +1 \quad \text{if} \quad 0 < \psi_1 - \chi_1 < \pi,$$

$$\epsilon = -1 \quad \text{if} \quad \pi < \psi_1 - \chi_1 < 2\pi.$$

The same formula has been obtained by Dronkers (1962) in his linearization of the quadratic resistance term of a purely sinusoidal tide.

2) THE OTHER WAVES IN THE SPECTRUM

For any frequency ω_k, $k \neq 1$, at the order of approximation A_1A_k, it is possible to deduce, from the development (8) presented in Le Provost (1973), quasi-linearized damping relations which take the form

$$\begin{cases} A_1A_kFX_{1k}^{(0)} \cos[\omega_k t + \phi X_{1k}^{(0)}] \\ \quad = (R_k + R_k')A_k u_k \cos(\omega_k t + \psi_k) \\ \qquad + R_k'' A_k v_k \cos(\omega_k t + \chi_k) \\ A_1A_kFY_{1k}^{(0)} \cos[\omega_k t + \phi Y_{1k}^{(0)}] \\ \quad = R_k'' A_k u_k \cos(\omega_k t + \psi_k) \\ \qquad + (R_k - R_k')A_k v_k \cos(\omega_k t + \chi_k), \end{cases} \tag{12}$$

with

$$R_k = \frac{3}{2}\frac{A_1}{\sqrt{2}}\sqrt{u_1^2 + v_1^2}\,G_{00},$$

$$R_k' = \frac{3}{2}\frac{A_1}{\sqrt{2}}\sqrt{u_1^2 + v_1^2}\,\frac{G_{02}}{2J_1}\frac{u_1^2 - v_1^2}{u_1^2 + v_1^2},$$

$$R_k'' = \frac{3}{2}\frac{A_1}{\sqrt{2}}\sqrt{u_1^2 + v_1^2}\,\frac{G_{02}}{2J_1}\frac{u_1 v_1}{u_1^2 + v_1^2}\cos(\chi_1 - \psi_1).$$

Thus, it appears that the damping terms corresponding to any component of index i in the spectrum can be written in the general linearized form

$$\begin{cases} ru_i + r'v_i \\ r''u_i + r'''v_i. \end{cases} \tag{13}$$

(i) For the dominant wave, limited at the approximation A_1^2:

$$r = r''' = \frac{C}{H}R_1; \quad r' = \frac{C}{H}\frac{R_1'}{\omega_1}\frac{\partial}{\partial t};$$

$$r'' = -\frac{C}{H}\frac{R_1'}{\omega_1}\frac{\partial}{\partial t}.$$

These coefficients depend on the dominant solution itself, but it must be noticed that, at this order of approximation, they are independent of the solution of the other waves in the spectrum.

(ii) For the other waves of index k limited to the order A_1A_k:

$$r = \frac{C}{H}(R_k + R_k'); \quad r' = r'' = \frac{C}{H}R_k'';$$

$$r''' = \frac{C}{H}(R_k - R_k').$$

These coefficients depend only on the dominant solution.

d. Modal equations defining any tidal constituent

It is useful to simplify the presentation and the computations, by using complex notation. The tidal potential (3) and the vector solution (5) are written as

$$\begin{cases} P_i \cos(\omega_i t + k_i) = \pi_i e^{j\omega_i t} \\ \qquad + \text{complex conjugate (c.c.)} \\ \zeta_{il} \cos(\omega_{il} t + \varphi_{il}) = \alpha_{il} e^{j\omega_{il} t} + \text{c.c.} \\ u_{il} \cos(\omega_{il} t + \psi_{il}) = \mu_{il} e^{j\omega_{il} t} + \text{c.c.} \\ v_{il} \cos(\omega_{il} t + \chi_{il}) = \nu_{il} e^{j\omega_{il} t} \\ \qquad + \text{c.c.} \quad (j^2 = -1). \end{cases} \tag{14}$$

Introducing the development (5) in Eqs. (1), using the expansion (8) for the non-analytical friction terms, and taking into account the quasi-linearized expressions (13) of the damping part of these terms, it is possible to deduce, for each frequency and each order of approximation of the perturbation method, a system of complex variables defining any tidal component:

$$(j\omega_{il} + r)\mu_{il} + (r' - f)\nu_{il} + \frac{g}{a\cos\phi}\frac{\partial \alpha_{il}}{\partial \lambda} = F_{\mu_{il}}, \tag{15a}$$

$$(r'' + f)\mu_{il} + (j\omega_{il} + r''')\nu_{il} + \frac{g}{a}\frac{\partial \alpha_{il}}{\partial \phi} = F_{\nu_{il}}, \tag{15b}$$

$$j\omega_{il}\alpha_{il} + \frac{1}{a\cos\phi} \times \left[\frac{\partial}{\partial \lambda}(H_{\mu_{il}}) + \frac{\partial}{\partial \phi}[H\nu_{il}\cos\phi)]\right] = F_{\alpha_{il}}, \tag{15c}$$

with $f = 2\Omega \sin\phi$. The right members $F_{\mu_{il}}$, $F_{\nu_{il}}$, $F_{\alpha_{il}}$ can be considered as forcing terms; they include for astronomical constituents the tide generating potential and for the nonlinear constituents the corresponding advective and frictional terms which produce harmonics and wave-wave interactions. For each system, the set of limit conditions is

$$\mathbf{V}_{il} \cdot \mathbf{n} = 0 \quad \text{on} \quad \Gamma_1 \tag{16a}$$

$$\alpha_{il} = [\alpha_{il}]_0 \quad \text{given along} \quad \Gamma_2. \tag{16b}$$

Several points must be noticed concerning (15):

1) For the dominant wave, the system (15) is limited to the first-order solution, but by including the damping terms (11), it is nonlinear because of the friction coefficients R_1 and R_1', which depend on the solution of the dominant wave itself. This problem will be solved through an iterative process, but independently of all the other constituents included in the real spectrum.

2) For any other component in the spectrum, of order A_k, the system (15), limited to the order A_1A_k and including the damping terms (12), is purely

linear, because the friction coefficients R_k, R_k' and R_k'' depend on the solution of the dominant wave only.

3) The complete resolution of problem (1) with limit conditions (2) will thus be solved as follows:

- First, the damped dominant wave solution, limited to the first-order A_1, is computed (through an iterative process).
- Second, any other astronomical constituent k is computed, at the order of approximation A_k, with a linearized bottom friction defined by the first-order approximation of the dominant wave, obtained previously.
- Third, a knowledge of all the astronomical components allows the computation of the nonlinear forcing terms F_μ, F_ν, F_α. Taking into account a linearized bottom friction as defined in (12), it is thus possible to determine any nonlinear shallow-water constituents: the second-order harmonics of the dominant wave as well as the second-order wave-wave interaction constituents.

4. General variational formulation and finite-element resolution

From (15a) and (15b), μ_{il} and ν_{il} can be solved as functions of the forcing terms and α_{ie}

$$\begin{cases} \mu_{il} = \dfrac{a}{H}\left[B\left(\dfrac{1}{\cos\phi}\dfrac{\partial\alpha_{il}}{\partial\lambda} - \dfrac{a}{g}F_{\mu_{il}}\right) - D\left(\dfrac{\partial\alpha_{il}}{\partial\phi} - \dfrac{a}{g}F_{\nu_{il}}\right)\right] & (17a) \\ \nu_{il} = \dfrac{a}{H}\left[A\left(\dfrac{\partial\alpha_{il}}{\partial\phi} - \dfrac{a}{g}F_{\nu_{il}}\right) - C\left(\dfrac{1}{\cos\phi}\dfrac{\partial\alpha_{il}}{\partial\lambda} - \dfrac{a}{g}F_{\mu_{il}}\right)\right] & (17b) \end{cases}$$

with the notation

$$A = (j\omega_{il} + r)E^{-1};\quad B = (j\omega_{il} + r''')E^{-1}$$
$$C = (r'' + f)E^{-1};\quad D = (r' - f)E^{-1}$$
$$E = a^2[\omega_{il}^2 + f^2 + f(r' - r'') + r'r'' - rr''' - j\omega_{il}(r + r''')](gH)^{-1}.$$

Substituting (17a) and (17b) in (15c), it is then possible to eliminate μ_{il} and ν_{il} and reduce the problem to the resolution of the equation

$$j\omega_{il}\cos\phi\alpha_{il} + \frac{\partial}{\partial\lambda}\left(\frac{B}{\cos\phi}\frac{\partial\alpha_{il}}{\partial\lambda} - D\frac{\partial\alpha_{il}}{\partial\phi}\right) + \frac{\partial}{\partial\phi}\left(A\cos\phi\frac{\partial\alpha_{il}}{\partial\phi} - C\frac{\partial\alpha_{il}}{\partial\lambda}\right) = F_{il}, \quad (17c)$$

where

$$F_{il} = F_{\alpha_{il}}\cos\phi + \frac{a}{g}\left\{\frac{\partial}{\partial\lambda}(BF_{\mu_{il}} - DF_{\nu_{il}}) + \frac{\partial}{\partial\phi}[(AF_{\nu_{il}} - CF_{\mu_{il}})\cos\phi]\right\}.$$

Thus, for each order of magnitude and frequency, we have to solve a second-order equation of the *Helmholtz* type relative to one complex unknown α_{il}, under limit conditions (16).

a. Variational formulation

We look for a solution of (17c) in a weak sense, that is, in the space $H^1(\mathcal{D})$ of complex-valued functions α, which real part α_r, imaginary part α_c and first partial derivatives are square integrable on the domain $\mathcal{D}$ of resolution. To do this, we integrate (17c) with a testing function β over the domain $\mathcal{D}$ and use a Green-Riemann formula in order to take into account the boundary conditions (16). Thus, we formulate the following variational problem

Find α in $H(\alpha_0)$, such that $L(\alpha, \beta) = F(\beta)$ holds for any β in $H(0)$, where $H(\alpha_0) = \{\alpha \in H^1(\mathcal{D});\ \alpha = \alpha_0 \text{ along } \Gamma_2\}$ and

$$L(\alpha,\beta) = \int_{\mathcal{D}}\left\{-j\omega\cos\phi\alpha\bar\beta + \frac{B}{\cos\phi}\frac{\partial\alpha}{\partial\lambda}\frac{\partial\bar\beta}{\partial\lambda} - D\frac{\partial\alpha}{\partial\phi}\frac{\partial\bar\beta}{\partial\lambda} + A\cos\phi\frac{\partial\alpha}{\partial\phi}\frac{\partial\bar\beta}{\partial\phi} - C\frac{\partial\alpha}{\partial\lambda}\frac{\partial\bar\beta}{\partial\phi}\right\}d\mathcal{D},$$

$$F(\beta) = \int_{\mathcal{D}}\left\{-F_\alpha\cos\phi\bar\beta + \frac{a}{g}\left[(BF_\nu - DF_\mu)\frac{\partial\bar\beta}{\partial\lambda} + (AF_\nu - CF_\mu)\cos\phi\frac{\partial\bar\beta}{\partial\phi}\right]\right\}d\mathcal{D}. \quad (18)$$

Index il has been omitted in these notations; $d\mathcal{D}$ denotes an element of area in $\mathcal{D}$. If we assume that the coefficients A, B, C, D, E are coefficients independent of the solution (which is not the case for the dominant wave), it is possible to prove the existence and the uniqueness of the solution, under some conditions of smoothness and orders of magnitude for the coefficients depending of friction, depth, and forcing terms F_μ, F_ν, F_α (Le Provost and Poncet, 1978; Poncet, 1979). Moreover, it can be shown that landward boundary conditions (16a) are automatically satisfied on Γ_1 by this solution.

b. Finite-element resolution

The variational problem (18) can be solved by a finite element method. Given a regular triangulation of $\mathcal{D}$, it is possible to use the classical results of Lagrange interpolation on triangles, in order to obtain an approximate solution to problem (18).

For practical applications, we used an automatic

finite-element package called DELTA built by Poncet (1979). Efficient in an interactive implementation, on a time-shared computer, it appears as a short language of commands allowing one to proceed through the different steps of formulation and resolution of a finite-element problem. This package has been adapted to the automatic computation of the principal harmonic constituents of the tide in a given area:

- The land boundaries are directly extracted from a library stored on a magnetic tape containing the description of the coasts all over the world.
- The depths are automatically interpolated at integration points from a bathymetric data base previously stored on a regular grid.
- Through the "domain" command of the code, it is possible to obtain an automatic triangulation of $\mathcal{D}$ with a specified size of the triangles along the boundaries.
- Through the "element" command of DELTA, various interpolation processes of the solution on the triangles are available. For practical applications we used Lagrange interpolation of first, second and third degrees.
- For each constituent in the spectrum, it is necessary to specify only its name, frequency, and complex sea surface elevation parameters along the open boundaries.
- When using a graphic display, the results are directly visualized on the screen: maps of isobaths, maps of triangulation of the domain, maps of equipotential lines for the amplitude and the phase of the sea level of the computed component, velocity field distribution in amplitude, and direction at the different phases of the studied period.

5. A numerical illustration

In order to illustrate the main characteristics of the method let us solve an idealized problem corresponding to the propagation of a tidal wave in a rotating channel of rectangular shape and constant depth. The time and space scales are chosen in reference to a schematic of a real basin which will be investigated in detail in the last section of this paper: the English Channel, which can be roughly approximated by a rectangular channel extending from 49 to 51°N, from 2°E to 5°W, with a constant depth of 50 m (see Fig. 1). Coastal conditions are considered at the east, north and south, and open sea boundary on the west. The wave coming from the ocean through the western limit is supposed to be monochromatic, of period 12 h 25 min (the M_2 component) but slightly distorted by its first harmonic M_4. However, an adequate boundary condition on the sea surface elevation is difficult to choose *a priori*, along the western limit. Thus, we decide to double the length of the channel and consider for this academic illustration a channel extending from 12°W to 2°E, in order to avoid, in the second half part of the basin, between 5°W and 2°E, most of the influence of open sea condition incoherences. The depth is taken constant (H = 50 m), and the limit conditions at the western boundary are arbitrarily chosen as constants: the amplitude ζ_{11} and the phase φ_{11} of the fundamental component, the amplitude ζ_{12} and the phase φ_{12} of its first harmonic. For the numerical experiment here presented, $\zeta_{11}(12°, \phi) = 4$ m, $\varphi_{11}(12°, \phi) = 0°$, $\zeta_{12}(12°, \phi) = 0.15$ m, $\varphi_{12}(12°, \phi) = 60°$; as will be seen later, the orders of magnitude of these data are in good agreement with in situ observations of the M_2 and M_4 constituents in the English Channel. The bottom friction coefficient is taken as 2.5×10^{-3}.

a. Resolution of the dominant wave limited to the first-order approximation

This fundamental component is supposed to be induced in the basin by the open boundary condi-

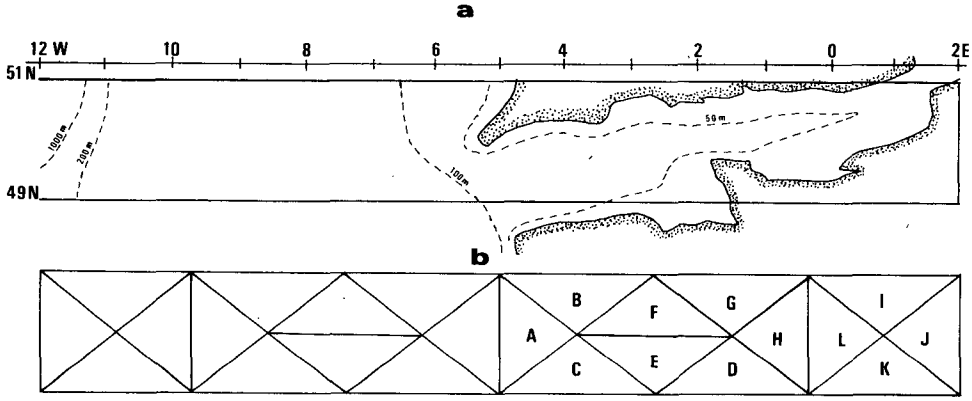

FIG. 1. Geographic location of the idealized channel considered (a) and triangulation used for the finite-element computations (b).

tions only (as usual in shallow-water areas, the tidal potential P is neglected; in the Channel, for instance, the maximum of amplitude of the M_2 tide forced by P is only of the order of 1 or 2 cm). Thus, the forcing terms of (15) disappear:

$$F_{\alpha 11} = F_{\mu 11} = F_{\nu 11} = 0.$$

For this dominant component, the coefficients of linearized friction R_1 and R_1' are those defined by (11), i.e., they are dependent on the solution itself. Consequently, we must solve a nonlinear problem, the solution for which is obtained through a classical iterative process. Starting from a guess for the velocity field $(\mu_{11})_0$ and $(\nu_{11})_0$, which fixes the values of the friction coefficients R_1 and R_1', we compute a first approximate solution of (15) through the variational problem (18), and then iterate until a satisfactory stability of the solution is obtained:

Step 1:

$$\left\{\begin{array}{l}\text{guess}\\(\mu_{11})_0\\(\nu_{11})_0\end{array}\right. \xrightarrow[(11)]{\text{from}} \left\{\begin{array}{l}(R_1)_1 = R_1[(\mu_{11})_0, (\nu_{11})_0]\\(R_1')_1 = R_1'[(\mu_{11})_0, (\nu_{11})_0]\end{array}\right.$$

$$\xrightarrow[\text{of (18)}]{\text{from solution}} \left\{\begin{array}{l}(\alpha_{11})_1\\(\mu_{11})_1\\(\nu_{11})_1\end{array}\right.$$

Step n:

$$\left\{\begin{array}{l}(\alpha_{11})_{n-1}\\(\mu_{11})_{n-1}\\(\nu_{11})_{n-1}\end{array}\right. \xrightarrow[(11)]{\text{from}} \left\{\begin{array}{l}(R_1)_n = R_1[(\mu_{11})_{n-1}, (\nu_{11})_{n-1}]\\(R_1')_n = R_1'[(\mu_n)_{n-1}, (\nu_{11})_{n-1}]\end{array}\right.$$

$$\xrightarrow[\text{of (18)}]{\text{from solution}} \left\{\begin{array}{l}(\alpha_{11})_n\\(\mu_{11})_n\\(\nu_{11})_n.\end{array}\right.$$

In order to accelerate the convergence of the iterative process, the Aitken scheme is applied, which consists in computing a new guess for the friction coefficients R_1 and R_1' before iterations number $n = 3k + 1$, following the formula:

$$G_n = S_n - [(S_{n-1} - S_n)^2/(S_{n-2} - 2S_{n-1} + S_n)]. \quad (19)$$

The numerical resolution of problem (18) is realized by using the finite-element procedure described previously. The triangulation is shown on Fig. 1; second-order elements are used to compute the α solution; the velocity field (μ, ν) is obtained from the α solution, using (17a) and (17b). Notice that second-order elements are necessary for the computation of α, in order to be sure of the convergence of its second-order derivatives, which must be known for the computation of the forcing advective terms in Eqs. (15). A first guess for the velocity field is necessary to begin the iterative process: one possibility is to take $(\mu_1)_0 = (\nu_1)_0 = 0$ (see Kabbaj and Le Provost, 1980). However, in the two-dimensional case it is better to fix a reasonable nonzero value for the velocity field, in order to obtain a reasonable solution as soon as the first iteration. An interesting simplification of formulas (10) and (11) arise when the hodograph of the current is rectilinear. In this case $J_1 = 1$, and so $R_1' = 0$, and R_1 is only a function of the maximum of the velocity, i.e.,

$$R_1' = (8/3\pi)V_{\max}. \quad (20)$$

In rather narrow channels, like the one here considered, the velocity vectors tend to be parallel to the lateral boundaries, except at the end of the channel. Thus, we choose the approximate value (20) as first guest for the iterative process, with $V_{\max} = 1$ m s^{-1}, which is the order of magnitude of the currents in areas like the English Channel.

The convergence of the iterative process is illustrated in Fig. 2. The amplitudes of the sea surface elevation and the longitudinal velocity component computed at the center of gravity of the triangles situated in the eastern half part of the channel are plotted for the different iterations. Seven iterations have been completed, with two accelerations following the Aitken scheme applied before iterations 4 and

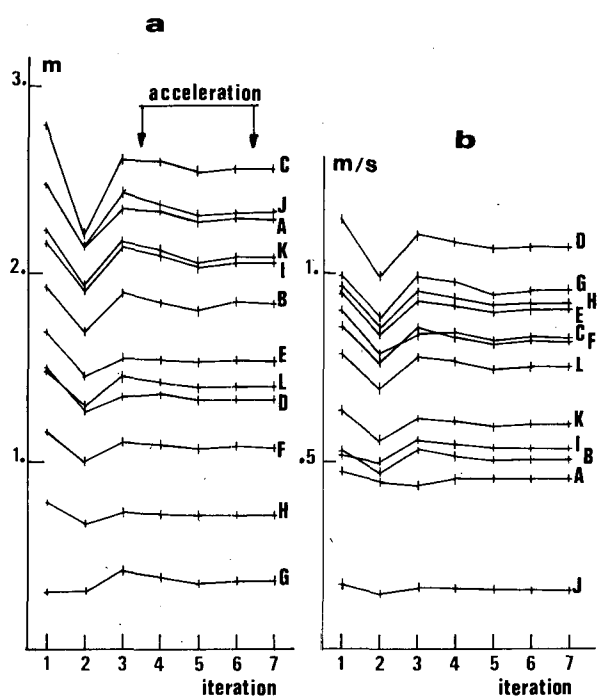

FIG. 2. Convergence of the iterative method of integration of (17), for the dominant wave, in the eastern half part of the academic channel, showing amplitudes of the sea surface elevation (a) and of the longitudinal component of the velocity (b), at the center of the different triangles. For geographic location of points A to L, see Fig. 1.

7, and it can be seen that the convergence is quite rapid. As early as the fourth iteration, just after the first Aitken acceleration, the solution is already quite good. It should be noticed that the limit solution obtained after these seven iterations (combined with two accelerations) is the same as the one obtained from a simple iterative procedure, without Aitken acceleration. In the latter case, 12 iterations are necessary to obtain the stable solution (see Rougier, 1979).

The cotidal lines of this solution are presented on Fig. 3. Given the depth of the channel and the period of the computed wave, it can be easily verified that the longitudinal size L of the channel corresponds to a wavelength of the oscillation. Consequently, the solution has two amphidromic points at the abscissa $L/4$ and $3L/4$. Because of friction damping, the western amphidromic point is virtual, the westward going reflected wave being much smaller than the incident wave. As was suspected, at the entrance of the channel the constant values of the amplitude and the phase of the wave is not coherent with the usual solutions in rotating systems; this is confirmed by the computed velocity field presented on Fig. 3c. Except at the entrance and the end of the channel, the velocities are quite parallel to the lateral boundaries. Near the end of the channel, the current roses are elliptic because of the wall at the eastern boundary. At the entrance of the channel, the horizontality of the sea surface, imposed by the limit condition $\zeta_{11} = C^{te}$, induces a velocity field curvature produced by the Coriolis force, not balanced in this area by any sea surface slope.

b. Resolution of the first harmonic of this dominant wave limited to the second-order approximation

Following the perturbation method presented in Section 3, the forcing terms F_α, F_μ and F_ν of this component are deduced from the advective terms of Eqs. (1a) and (1b), and the nonlinear term of (1c):

$$\begin{cases} F_{\mu_{12}} = -\dfrac{1}{a\cos\phi}\left[\mu_{11}\dfrac{\partial\mu_{11}}{\partial\lambda} - \nu_{11}\dfrac{\partial}{\partial\phi}(\mu_{11}\cos\phi)\right], & \text{(21a)} \\ F_{\nu_{12}} = -\dfrac{1}{a\cos\phi}\left[\mu_{11}\dfrac{\partial\mu_{11}}{\partial\lambda} + \nu_{11}\dfrac{\partial\nu_{11}}{\partial\phi}\cos\phi + \mu_{11}^2\sin\phi\right], & \text{(21b)} \\ F_{\alpha_{12}} = -\dfrac{1}{a\cos\phi}\left[\dfrac{\partial}{\partial\lambda}(\alpha_{11}\mu_{11}) + \dfrac{\partial}{\partial\phi}(\alpha_{11}\nu_{11}\cos\phi)\right]. & \text{(21c)} \end{cases}$$

The associate friction terms are defined by (12), functions of the solution of the dominant wave only and, consequently, known from the preceding

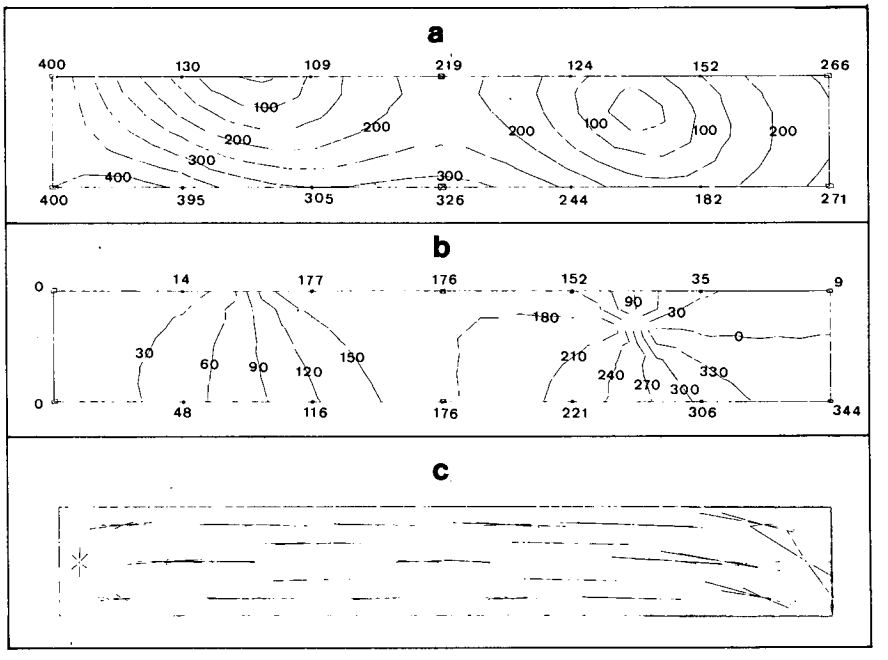

FIG. 3. Idealized channel. Solution for the dominant wave limited to the first-order approximation showing distribution of the (a) amplitude (cm) of the sea surface elevation (b) cotidal lines (deg), and velocity vectors at time 2, 4, 6, 8, 10 and 12 h.

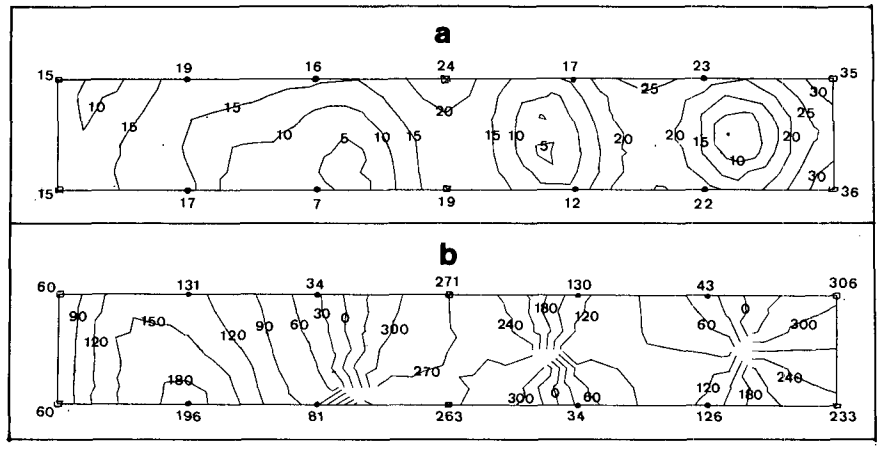

FIG. 4. Idealized channel. Solution for the first harmonic of the dominant wave limited to the second-order of approximation showing (a) distribution of amplitudes (cm) and (b) cotidal lines (deg).

computations:

$$R_2 = R_2(\mu_{11}, \nu_{11}); \quad R_2' = R_2'(\mu_{11}, \nu_{11});$$
$$R_2'' = R_2''(\mu_{11}, \nu_{11}). \tag{22}$$

Thus, for this harmonic constituent, the problem (15) is purely linear and can be solved easily through the variational formulation (18) by using the finite-element procedure already used for the dominant solution, but here without any iterative process. An arbitrary set of conditions is taken as the open boundary: $\zeta_{12} = 15$ cm, $\varphi_{12} = 60°$.

The results are presented in Fig. 4. As expected, real amphidromic points, at a distance of $L/4$, are found in the eastern part of the channel. Three real points appear, while a rather confusing pattern occupies the first quarter of the channel, near the open boundary. The location of the eastern amphidromic point, just at the same distance from the two lateral boundaries, proves that in this area the wave going eastward has the same amplitude as the one propagating westward. In contrast, the western point is near the southern boundary: in this area the part of the harmonic propagating toward the output of the channel is larger than the one in the other direction, which is easily understood because an important part of the energy is given inside the channel by nonlinear transfers from the fundamental wave, and then propagated outside.

6. Example of practical application: The tides in the English Channel

The English Channel is an excellent area for testing our method, because Chabert d'Hières and Le Provost (1979) have published an atlas of the main components of the tide in that domain, established from an extensive study based on *in situ* observation, and data obtained from a reduced physical model of that sea, built on a rotating platform. Thus, the solutions are already well known and give us the possibility of checking our numerical simulations. The procedure is the same as the one

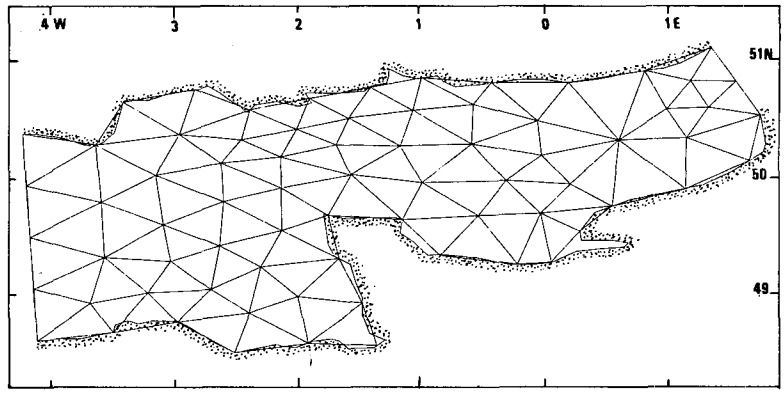

FIG. 5. Triangulation used for the English Channel.

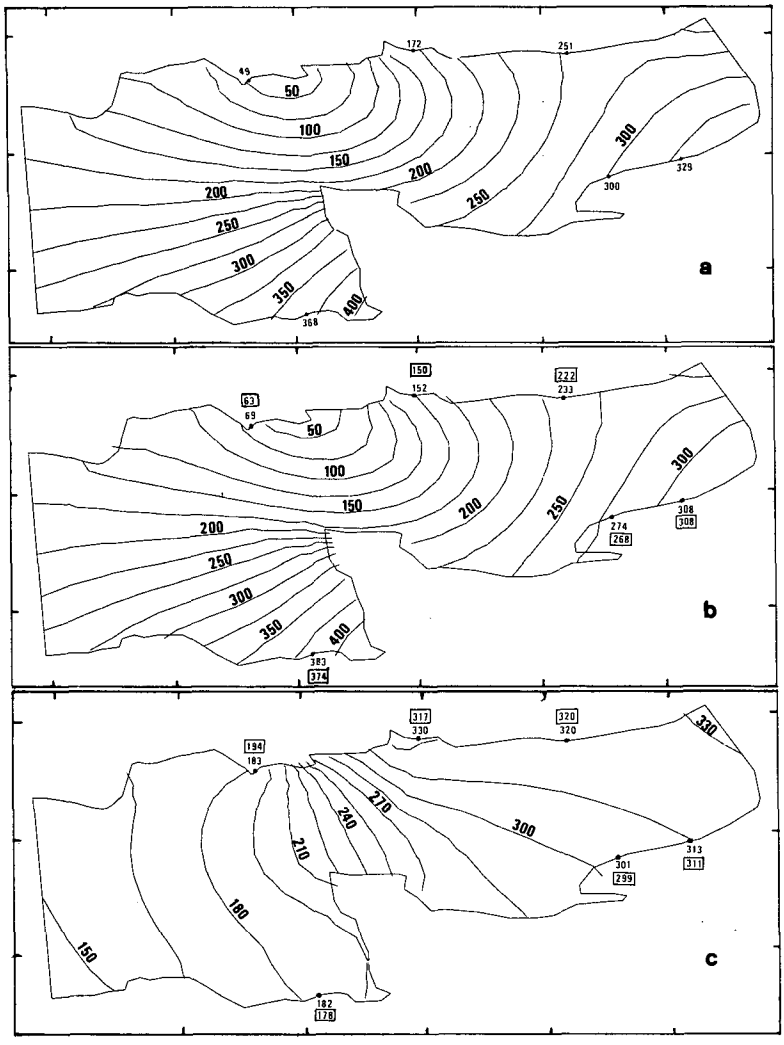

FIG. 6. The English Channel. Solution of the M_2 tides showing coamplitude lines (cm) after the first interation (a) and the seventh iteration (b); and cophase lines (deg) after the seventh iteration (c). Computed values are given at some particular nodes, to be compared with *in situ* observed values placed in brackets.

followed in the preceding section. The first step is the computation of the dominant wave M_2.

a. The dominant wave M_2

The domain investigated is limited by a line Devonport-Roscoff as the western boundary and Boulogne-Douvres as the eastern boundary. The description of the coastal limits are obtained from the library describing the World Ocean limits, already mentioned in Section 3b (Fig. 5). A network of 110 triangles is built automatically, with a regular discretization of the coastal line by elements of 45 km (this triangulation is coarse and could be refined, but we shall see that even with this limited number of triangles, the solutions are satisfying). The depths at integration points are interpolated from a data base of 264 nodes distributed on a regular rectangular network with 1/6° in longitude and 1/9° in latitude. As limit conditions, we know exactly, from harmonic analysis of *in situ* observation in Devonport (Dt), Roscoff (R), Boulogne (B) and Douvres (Ds), the amplitude and the phase of M_2. Thus, in a first approach, we have carried our computations with a definition of α along the open limits Dt − R and B − Ds deduced by a linear interpolation between the known values at the *in situ* observation points. The results presented in the following have been obtained from an exponential interpolation between Dt and R, which is in better agreement with the solution obtained by Chabert d'Hières and Le Provost (1979). As a first estimate of the friction coefficients, we take $R_1' = 0$ and $R_1' = (8/3\pi)V_{\max}$

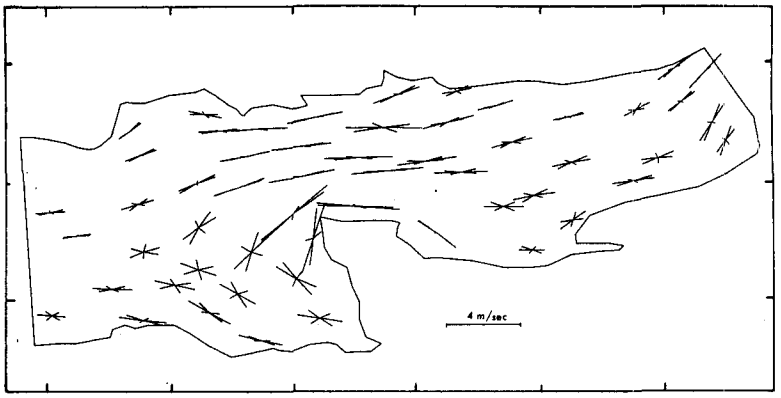

FIG. 7. The English Channel. Computed velocity vectors for the M_2 tide, at the center of gravity of some triangles, every 2 h.

with $V_{max} = 1$ m s^{-1}, just as for the academic channel previously considered. C is fixed to its classical value of 2.5×10^{-3}. Second-order elements are used for the computation of α by our FEM procedure, and seven iterations are sufficient to obtain a stable solution.

Coamplitude lines are presented for the first and seventh iterations (Figs. 6a and 6b respectively). Compared to the solution of Chabert d'Hières and Le Provost (1979) the first estimate already looks good, but a detailed examination of the solution shows that the amplitude of the wave is too big in the eastern part of the basin, and that the minimum of amplitude is not correctly situated (displaced toward the west). After only the second iteration (not presented here), the results are efficiently corrected, leading to a wave slightly too damped, as can be expected from the iterative process; the final solution presented in Fig. (6b) is satisfying, within 3% of difference with the values deduced from *in situ* observations along the coasts.

Fig. 6c gives the computed cophase solution, in good agreement with the observed values (in brackets). In Fig. 7, current vectors are presented

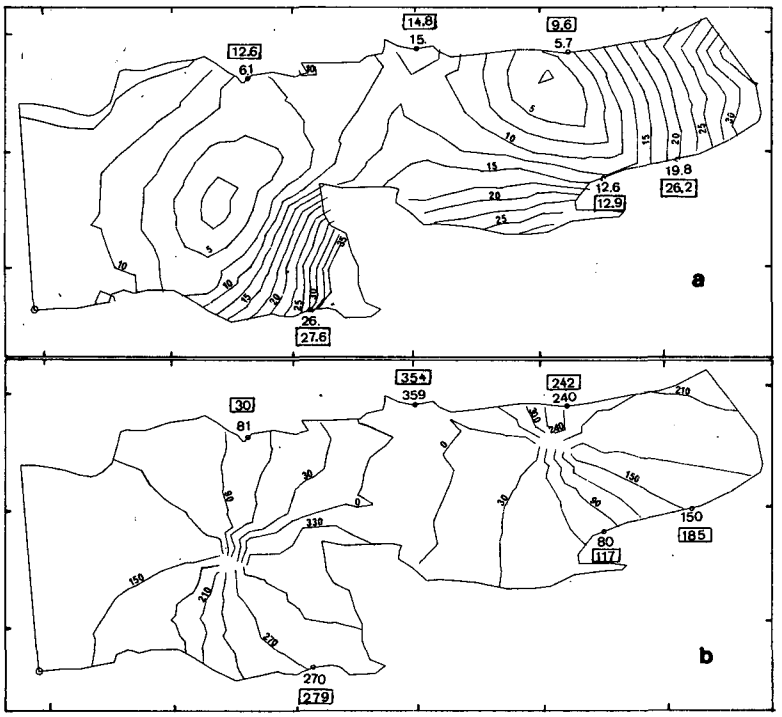

FIG. 8. The English Channel. Cotidal lines for the harmonic M_4 showing (a) amplitudes (cm) and (b) phases (deg).

TABLE 1. Name, symbol, period and relative amplitude of the main constituents of the tide generating potential.

i	Name (semidiurnal)		Period (h/min)	P_i/P_1
1	Principal lunar	M_2	12/25	1
2	Principal solar	S_2	12	0.4653
3	Major elliptical lunar	N_2	12/39	0.1936
4	Luni-solar declinational	K_2	11/59	0.1267
5	Minor elliptical lunar	L_2	12/11	0.0422
6	Evictional major	ν_2	12/37	0.0375
7	Variational	μ_2	12/52	0.0306
8	Major elliptical solar	T_2	12/01	0.0273
9	Second-order elliptical lunar	$2N_2$	12/54	0.0259
10	Evictional minor	λ_2	12/13	0.0073
	(diurnal)			P_i/P_{11}
11	Luni-solar declinational	K_1	23/56	1
12	Principal lunar	O_1	23/49	0.7110
13	Principal solar	P_1	24/03	0.3309
14	Major elliptical lunar	Q_1	26/56	0.1376

at the center of gravity of some of the triangles; we can notice the intensification of the velocity in the central part of the channel, especially around the La Hague Cap. In this area, the velocity field is quite rectilinear. In contrast, in the Bay of Mont St. Michel and in the eastern part of the basin, the hodographs are elliptic because of the influence of the coastal topography and the effect of the Coriolis force. Near the Strait of Dover, these hodographs are rectilinear because of the narrow passage between England and France. All these details are in good agreement with observed currents.

b. The nonlinear first harmonic wave M_4 of the dominant wave M_2

Following the method presented in this paper and illustrated in the Section 5, we have computed the M_4 constituent produced by the M_2 wave on the continental shelf. The forcing terms (21) and damping coefficients (22) are computed from the M_2 solution obtained previously. Some difficulties arise for the choice of limit conditions along Dt – R and B – Ds, because of the lack of observed values away from the coasts. In a first attempt, a linear interpolation of ζ_{12} and φ_{12} between the known values at Dt, R, B and Ds led to an incorrect solution in the western part of the domain. A more precise definition of ζ_{12} along the limit Dt – R has consequently been deduced from the known solution of Chabert d'Hières and Le Provost (1979), following an exponential distribution from the French coast to the English coast. The corresponding solution is presented in Fig. 8. Two amphidromic points appear, one in the western part and the other in the eastern basin, with phases propagating toward the west along the western coast of England, and toward the east along the eastern coast, just as observed *in situ*. Some imprecision still remains, but this solution, obtained with a rather coarse triangulation (cf. Fig. 5), is in good agreement with the Chabert d'Hières and Le Provost solution.

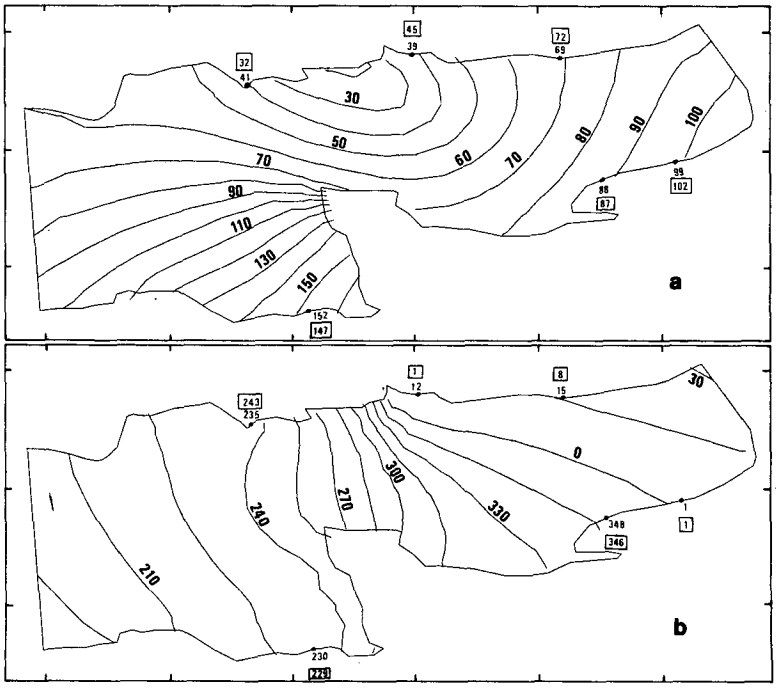

FIG. 9. As in Fig. 8 except for the semidiurnal S_2 tide.

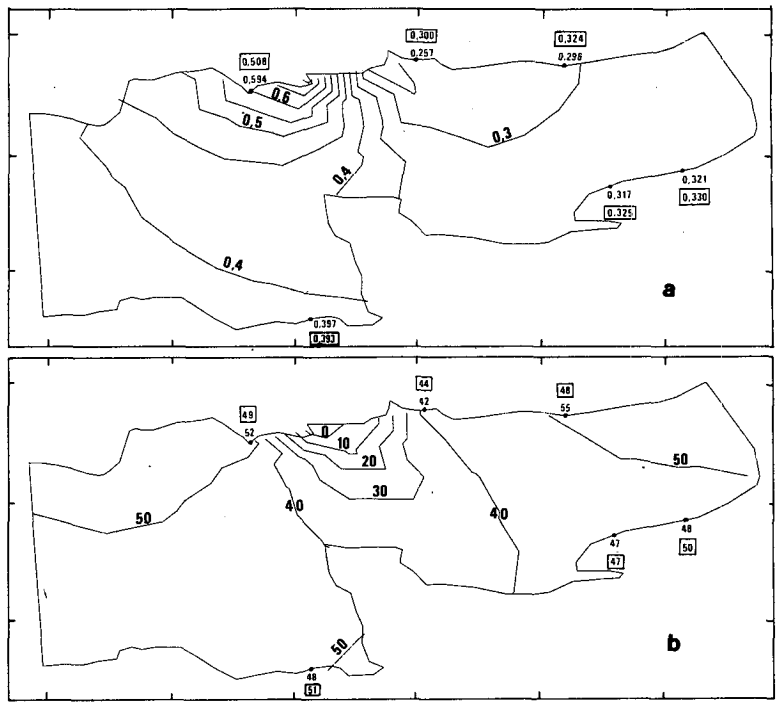

FIG. 10. The English Channel. Comparison of the M_2 and S_2 solutions showing S_2/M_2 ratios (a), and ($S_2 - M_2$) phase differences (b).

An important point must be noticed from this M_4 computation. It appears that such a solution is very sensitive to the definition of open-sea limit conditions. Thus, if open sea *in situ* values are not available, we must take care to locate the marine boundaries as far as possible from the nonlinear shallow-water areas. We must mention that the spectral finite-element method presented in this paper could be adapted to the investigation of an optimized set of open-sea boundary conditions, based on the comparison of computed and observed values along the coasts of the studied domain.

c. The other waves in the spectrum

Following the present method, the computation of the main astronomical constituents (S_2, N_2, K_2, . . . , K_1, O_1) corresponds to the resolution of linear problems of type (18), because friction coefficients R_k, R_k' and R_k'' depend on the dominant solution only, if limited at the order A_1A_k [see Eq. (12)].

As examples of results, the computed cotidal charts of two astronomical constituents are presented: S_2, which is the main solar contribution in the semidiurnal species, and K_1, which is the principal diurnal constituent in the Channel. In Fig. 9 it can be seen that the S_2 solution is qualitatively very similar to the M_2 solution, because of the proximity of their situation in the spectrum. However, the differences between these solutions are significant. In Fig. 10 the distribution of the S_2/M_2 ratios and ($S_2 - M_2$) phase differences are presented. These nets are typical and have already been interpreted by Le Provost (1974) when he compared the similar solutions obtained in his intensive study of the main components of the tides in this area. These figures are characteristic of the difference of wavelength between the two constituents: as these waves are partly reflected by the Picardy coast on the east side of the domain, an estimate of the position of their minimum of amplitude, along the English coast, can be made through the computation of a quarter of their wavelength, from the eastern side of the model, toward the west. As their wavelengths are proportional to their period, we deduce that the amphidromic point of the M_2 wave, of longer period, is situated to the west of the S_2 amphidromic point. This explains the increase of the S_2/M_2 ratio in the area of minimum of M_2 amplitude, and the rapid decrease of this ratio toward the east; in the same way, a rapid change of the ($S_2 - M_2$) difference of phase is observed around this area of minimum of amplitude of the two waves, resulting from the difference in position of their (virtual) amphidromic points.

Fig. 11 gives the cotidal charts computed for the K_1 constituent; this diurnal solution is completely different from the M_2 and S_2 semidiurnal solution, with an amphidromic point near the Strait of Dover.

All these results are in good agreement with *in situ* observations.

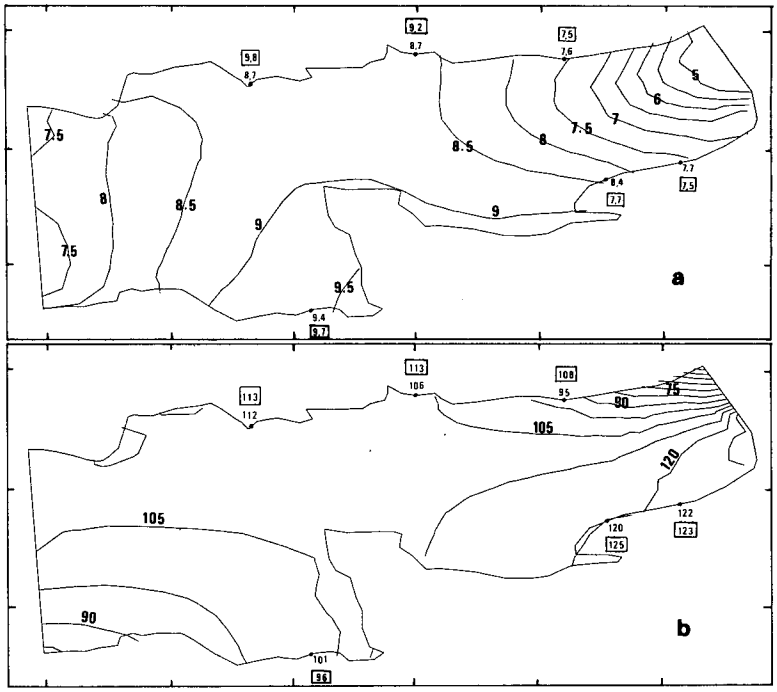

FIG. 11. As in Fig. 8 except for the diurnal-K_1 tide.

7. Conclusions

We cannot present here other results because of lack of space, but the procedure is the same for all the other astronomical or nonlinear constituents. If the investigated area is not restricted to very shallow-water areas, the present method is well adapted to give satisfying solutions for the main constituents of the tide, with very low computing time requirements. For the English Channel, a comparison of computer costs on IBM 360/65 has been performed between our present in time-spectral FEM, and a classical second-order FDM solving the time-dependent hyperbolic problem (1) and giving similar results.

The FEM has been applied with the triangulation presented in Fig. 5, with second-order elements and seven points of numerical integration taken on each triangle. The FDM is based on a predictor-corrector second-order scheme, with an elementary mesh of 10 km. In order to avoid excessive computer expenses, we have limited the tidal cycle to the semi-monthly modulation, i.e., simplified the semidiurnal astronomical spectrum to M_2 and S_2. Thus, we know from previous investigations (Le Provost, 1974) that the corresponding nonlinear spectrum in the Channel can be correctly described by looking at the constituents

$$M_2,\ S_2,\ 2\,MS_2,\ 2\,SM_2,\ M_4,\ MS_4,\ 3\,MS_4,\ M_6,\ 2\,MS_6.$$

With the FEM, one iteration for the dominant wave needs 50 s. Since seven iterations are used for the M_2 computation, its cost is 350 s. The computation of any other astronomical constituent takes 32 s. The determination of a nonlinear constituent, such as M_4, needs 50 s. Thus, the total cost is $50 \times 7 + 32 + 50 \times 7 = 732$ s, i.e., ~12 min.

The second-order FDM which we used needs four semidiurnal tidal periods to reach stability, and then must be run for half a month, i.e., 29 periods. Since one period of simulation needs 336 s, the total cost of such a simulation is $(4 + 29) \times 336 = 11\,088$ s, i.e., ~3 h.

The comparison of these two times shows that our spectral FEM is 15 times faster for this particular example. Thus, given the other interesting characteristics of the model (flexibility of the size of the triangulation, automation of the resolution, stability, . . .) this method appears to be attractive for studying tides in oceanic or shallow-water areas.

Acknowledgments. This work has been supported by the National Center of Scientific Research under Contract A.T.P. 2994 and by the National Center for Oceans Exploitation under Contract 78/1967.

REFERENCES

Brebbia, C. A., and P. W. Partridge, 1976: Finite-element simulation of water circulation in the North Sea. *J. Appl. Math. Model*, **1**, 101–107.

Brettschneider, G., 1967: Anwendung der Hydrodynamisch numerischen Verfahrens zur Ermittlung der M_2. Mitschwin-

gungsgezeit der Nordsee, Mittl. Inst. Meereskunde, University of Hamburg, No. 7.

Chabert d'Hières, G., and C. Le Provost, 1979: Atlas des composantes harmoniques de marée dans la Manche. *Ann. Hydrogr.*, **6,** No. 3, 5–36.

Connor, J. J., and J. D. Wang, 1974: Finite element modeling of hydrodynamic circulations. *Numerical Methods Fluid Dynamics,* Pentech Press, 355–367.

Darwin, G. H., 1883: Report on harmonic analysis of tidal observations. *Brit. Assoc. Adv. Sci. Rep.*, 48–118.

Davies, A. M., 1976: A numerical model of the North Sea and its use in choosing locations for the deployment of offshore tide gauges in the Jonsdap' 76 oceanographic experiment. *Sonderbruck Dtsch. Hydrogr. Z.*, **29,** No. 1, 11–24.

Doodson, A. T., 1921: The harmonic development of tide generating potential. *Proc. Roy. Soc. London*, **A100,** 305–328.

Dronkers, J. J., 1962: The linearization of the quadratic resistance terms in the equation of motion of a pure harmonic tide in a sea. *Proc. Symp. Math. Hydrodyn. Math. Phys. Ocean.,* Institute fur Meercskunde der Universität Hamburg.

Flather, R. A., 1976: A tidal model of the northwest European continental shelf. *Mém. Soc. Roy. Sci. de Liège*, Ser. 6, **10,** 141–164.

Gray, W. G., 1980: Do finite element models simulate surface flow? Manuscript, Princeton.

Grotkop, G., 1973: Finite element analysis of long-period water waves. *Comput. Methods Appl. Mech. Eng.*, **2,** 147–157.

Hansen, W., 1962: Hydrodynamical methods applied to oceanographic problems. *Proc. Symp. Math. Hydrodyn. Phys. Ocean.,* Institut fur Meercskunde der Universität Hamburg, 24–34.

Heaps, N. S., 1974: Development of a three-dimensional numerical model of the Irish Sea. *Rapp. P.V. Reun. Cons. Int. Explor. Mer*, **167,** 147–162.

Jamart, B. M., and D. F. Winter, 1978: A new approach to the computation of tidal motions in estuaries. *Hydrodynamics of Estuaries and Fjords, Elsevier Oceanography Series,* Vol. 23, 261–281.

Kabbaj, A., and C. Le Provost, 1980: Nonlinear tidal waves in channels: A perturbation method adapted to the importance of quadratic bottom friction. *Tellus*, **32,** 143–163.

Kawahara, M., and K. Hasegawa, 1978: Periodic Galerkin finite element method of tidal flow. *Int. J. Num. Methods Eng.*, **12,** 115–127.

——, —— and Y. Kawanago, 1977: Periodic tidal flow analysis by finite element perturbation method. *Comput. Fluids*, **5,** 175–189.

Hyacinthe, J. L., and J. Kravtchenko, 1970: Modèle mathématique des marées littorales: Calcul numérique sur l'exemple de la Manche. *La Houille Blanche*, No. 6, 639–650.

Le Provost, C., 1973: Décomposition spectrale du terme quadratique de frotement dans les équations des marées littorales. *C.R. Acad. Sci.*, **276,** 571–574, 653–656.

——, 1974: Contribution à l'étude des marées dans les mers littorales. Application à la Manche. Thèse d'état, Université de Grenoble, 228 pp.

——, and A. Poncet, 1977: Sur une méthode numérique pour calculer les marées océaniques et littorales. *C.R. Acad. Sci.*, **B285,** 349–352.

——, and ——, 1978: Finite-element method for spectral modelling of tides. *Int. J. Num. Methods Eng.*, **12,** 853–871.

Lynch, D. R., 1978: Finite element solution of shallow water equations. Ph.D. thesis, Princeton University.

Martchuk, G. I., R. G. Gordeev and V. Y. Rikving, 1973: A numerical method for the solution of tidal dynamics equations and the results of its application. *J. Comput.*, **13.**

Nihoul, J. C., and F. C. Ronday, 1975: The influence of the tidal stress on the residual circulation. *Tellus,* **29,** 484–490.

Pearson, C. E., and D. F. Winter, 1977: On the calculation of tidal currents in homogeneous estuaries. *J. Phys. Oceanogr.*, **7,** 520–531.

Pingree, R. D., and L. Maddock, 1978: The M_4 tide in the English Channel derived from a non-linear numerical model of the M_2 tide. *Deep-Sea Res.*, **25,** 53–63.

Poncet, A., 1979: Autour de l'écriture d'un code d'éléments finis. Thèse d'état, Université de Grenoble.

Prandle, D., 1978: Residual flows and elevations in the southern North Sea. *Proc. Roy. Soc. London*, **A359,** 189–228.

Rougier, G., 1979: Modélisation spectrale des marées dans les mers littorales. Thèse de 3ème Cycle, Université de Grenoble, 139 pp.

Ramming, H. G., 1976: A nested North Sea model with fine resolution in shallow coastal areas. *Mém. Soc. Roy. Liège*, **10,** 9–26.

Taylor, C., and J. M. Davis, 1975: Tidal propagation and dispersion in estuaries. *Finite Elements in Fluids*, Vol. 1, Wiley, Chap. 5.

Wang, J. D., 1978: Real time flow in unstratified shallow water. *J. Waterway Port, Coastal and Ocean. Div., ASCE*, **104,** 53–68.